Theoretical and Applied Mechanics Letters 5 (2015) 1–4

Contents lists available at ScienceDirect

Theoretical and Applied Mechanics Letters

journal homepage: www.elsevier.com/locate/taml

Letter

# Adjoint-based optimization of flapping plates hinged with a trailing-edge flap

Min Xu [a], Mingjun Wei [a,*], Chengyu Li [b], Haibo Dong [b]

[a] New Mexico State University, Las Cruces, NM 88003, USA
[b] University of Virginia, Charlottesville, VA 22904, USA

ARTICLE INFO

*Article history:*
Received 24 November 2014
Accepted 1 December 2014
Available online 3 February 2015
*This article belongs to the Fluid Mechanics

*Keywords:*
Flapping wing
Trailing-edge flap
Adjoint-based optimization

ABSTRACT

It is important to understand the impact of wing-morphing on aerodynamic performance in the study of flapping-wing flight of birds and insects. We use a flapping plate hinged with a trailing-edge flap as a simplified model for flexible/morphing wings in hovering. The trailing-edge flapping motion is optimized by an adjoint-based approach. The optimized configuration suggests that the trailing-edge flap can substantially enhance the overall lift. Further analysis indicates that the lift enhancement by the trailing-edge flapping is from the change of circulation in two ways: the local circulation change by the rotational motion of the flap, and the modification of vortex shedding process by the relative location between the trailing-edge flap and leading-edge main plate.



The unsteady aerodynamic phenomena that allows insects to operate efficiently at low-Reynolds-number is produced by flapping-wing mechanism. The inherently unsteady nature of flapping-wing kinematics is responsible for the primary force production [1], and also differentiates flapping-wing motion from conventional fixed and rotary wing configurations. In recent years, more attention has been paid to the aerodynamics of deformable wings [2,3]. Results have revealed that the dynamically changed wing surface, either actively or passively deformed, would potentially provide new aerodynamic mechanisms [4] of force productions over completely rigid wings [1,5] in flapping flights. The performance of a rigid wing can be significantly improved by adding chord-wise flexibility onto the wing. Vanella et al. [6] used a 2-D two-link model to model the chord-wise flexibility in a flapping plate. It shows that if appropriately chosen, the chord-wise flexibility can result in up to 28% enhancement in terms of lift-to-drag ratio and 39% increase for lift-to-power ratio comparing to a rigid one. In addition, Wan et al. [7] investigated the effect of chord-wise flexibility over a range of hovering kinematics parameters using a hinged-plate model. Their results indicated that higher lift-to-drag ratio can be obtained by hinging the plate at three-quarter chord from the leading-edge comparing to a fully rigid plate in the same flapping kinematics. Li et al. [8] performed numerical simulations of deformable flapping plate by attaching a trailing-edge flap (TEF) and studied its effects on aerodynamic performance and flow modulation. Results have shown that the optimal lift production can be achieved by tailoring the trailing-edge deflection angle and phase shift. The enhancement of lift production is up to 26% comparing to a completely rigid flapping plate.

However, if the parameter space of the problem is further increased, it is impracticable to find the optimal setting via direct parametric case study. Adjoint-based optimization, on the other hand, offers the same computational efficiency for increased number of control parameters [9–11]. In this work, we have developed an adjoint-based approach to quickly find the optimal solution of chord-wise wing morphing. The further analysis of the optimal solution allows us to study the effect of wing flexibility through its comparison to rigid and other configuration not optimized for aerodynamic performance. The rest of the paper is arranged in the following manner. The governing equations and numerical simulation details are first introduced. Then, the optimization results are discussed. The conclusion is given at the end.

Shown in Fig. 1, the configuration of the flapping plates is chosen to be the same as the one used by Li et al. [8], which allows a convenient comparison of performance and accuracy from different approaches. The leading-edge (i.e. main) plate and the trailing-edge plate are respectively 0.75 and 0.25 based on the total length. The flapping motion is prescribed by

$$\begin{aligned} x_{\mathrm{L}}(t) &= \frac{A_{\mathrm{L}}}{2}(1+\cos 2\pi ft), \qquad y_{\mathrm{L}}(t) = 0, \\ \theta_{\mathrm{L}}(t) &= \beta_{\mathrm{L}} \sin(2\pi ft), \\ \theta_{\mathrm{T}}(t) &= \beta_{\mathrm{T}} \sin(-2\pi ft + \varphi_{\mathrm{T}}), \end{aligned} \tag{1}$$

* Corresponding author.
*E-mail address:* mjwei@nmsu.edu (M. Wei).

http://dx.doi.org/10.1016/j.taml.2014.12.005

where $A_L = 3$ and $\beta_L = 45^\circ$ are respectively the amplitudes of the leading-edge plate's horizontal and rotational motion, and $f = 1/(3\pi)$ is the flapping frequency. All the variables are non-dimensionalised by the total chord-length $c$ and the reference velocity $U_{ref} = \pi f A_L$. The control parameters are the flapping amplitude $\beta_T$ and the phase delay $\varphi_T$ of the trailing-edge flap. The two parameters are optimized to achieve the maximum lift. The Reynolds number, $Re = U_{ref}c/\nu$, is 100 for all the cases. Here, we only consider the periodic state, which can be achieved after 8 flapping cycles.

The surrounding flow satisfies the incompressible Navier–Stokes equations

$$\begin{aligned} &\frac{\partial u_j}{\partial x_j} = 0, \\ &\frac{\partial u_i}{\partial t} + \frac{\partial u_j u_i}{\partial x_j} + \frac{\partial p}{\partial x_i} - \nu \frac{\partial^2 u_i}{\partial x_j^2} = 0, \end{aligned} \tag{2}$$

with convective boundary conditions at the far field, and the Dirichlet condition along the solid wing surface $\mathcal{S}$

$$u_i = V_i \quad \text{on } \mathcal{S}, \tag{3}$$

where $V_i$ is the local velocity of solid.

Staggered Cartesian mesh with local refinement through stretching is used to provide both efficiency and numerical stability. Immersed boundary method [12,13] is implemented for the description of moving solid boundaries (i.e. hinged plates) in both the forward simulation of fluid flow and the backward simulation of the adjoint field. The second-order central difference scheme is used for spatial discretization and the third-order Runge–Kutta/Crank–Nicolson scheme is used for time advancement [14–16]. The continuity equation for incompressible flow is enforced by projection method [16].

The computational domain has non-dimensional size $30 \times 30$. A stretched $290 \times 320$ Cartesian mesh is used for an overall Eulerian description of the combined fluid and solid domain. The grid is clustered near solid region with a minimum size of $\Delta x = \Delta y = 0.02$. There are 202 marker points for the Lagrangian description of the moving hinged plates with zero thickness.

Among many aerodynamic performance metrics, for demonstration, lift coefficient $C_l$ is picked in this work as the objective function, $\mathcal{J} = C_l$, to achieve the optimal lift performance. The control $\phi = (\beta_T, \varphi_T)$ has two parameters which are optimized to maximize the cost function. For problems involving moving solid boundaries (or morphing domain), it has been demonstrated that non-cylindrical calculus [17,18] has great advantages in efficiency and simplicity in the derivation of an adjoint equation in continuous form [14,15]. Following the same derivation, we get the adjoint equation in its continuous form as

$$\begin{aligned} &\frac{\partial u_j^*}{\partial x_j} = 0, \\ &\frac{\partial u_i^*}{\partial t} + u_j \left( \frac{\partial u_i^*}{\partial x_j} + \frac{\partial u_j^*}{\partial x_i} \right) + \frac{\partial p^*}{\partial x_i} + \nu \frac{\partial^2 u_i^*}{\partial x_j^2} = 0, \end{aligned} \tag{4}$$

with boundary conditions

$$\frac{\partial p^*}{\partial n} = 0, \quad \text{and} \quad u_i^* = -\delta_{i2} \quad \text{on } \mathcal{S}, \tag{5}$$

where $\delta_{ij}$ is Kronecker's delta. The adjoint equation then can be solved backward in time to provide the gradient/sensitivity for the optimization of cost function. Because of its similarity to the forward flow equation, the adjoint equation is discretized and solved similarly by numerical algorithms for the forward solver as disscussed earlier. The adjoint field eventually reaches periodic state by no more than 3 flapping cycles.

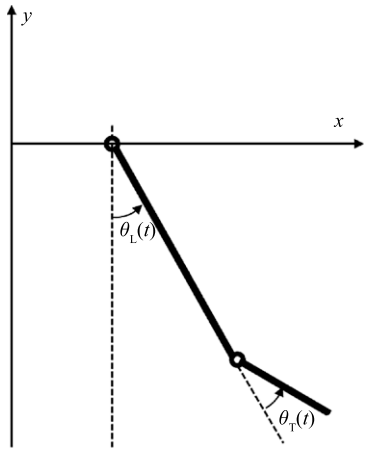


**Fig. 1.** Schematic of a flapping plate hinged with a trailing-edge flap.

Solving forward the flow equation and backward the adjoint equation, we get the flow solution $(u_i, p)$ and the adjoint solution $(u_i^*, p^*)$, which together provide the gradient of the cost function $\mathcal{J}$ with respect to the control $\phi$

$$\begin{aligned} \frac{\partial \mathcal{J}}{\partial \phi_l} = \frac{2}{\rho U_{ref}^2 cT} \int_{T_0}^{T_0+T} \int_{\mathcal{S}} \Bigg[ & Z_{k,l} \frac{\partial \sigma_{2j}}{\partial x_j} n_k \\ & - \left( \dot{V}_{i,l} - Z_{k,l} \frac{\partial u_i}{\partial x_k} \right) \left( \sigma_{ij}^* n_j + u_j^* u_j n_i \right) \Bigg] \mathrm{d}s\mathrm{d}t, \end{aligned} \tag{6}$$

where

$$\begin{aligned} &\dot{V}_{i,l} = \frac{\partial V_i}{\partial \phi_l}, \qquad Z_{i,l} = \frac{\partial S_i}{\partial \phi_l}, \\ &\sigma_{ij} = -p\delta_{ij} + \nu \left( \frac{\partial u_i}{\partial x_j} + \frac{\partial u_j}{\partial x_i} \right), \\ &\sigma_{ij}^* = p^* \delta_{ij} + \nu \left( \frac{\partial u_i^*}{\partial x_j} + \frac{\partial u_j^*}{\partial x_i} \right), \end{aligned} \tag{7}$$

and $S_i$ is the location of the solid point, $n_i$ is the norm direction from solid to fluid and $T$ is the time for one flapping cycle. The control is updated along the gradient to eventually converge to an optimal solution. The accuracy of the gradient computed by adjoint approach has been validated in our earlier work, and there are also details on derivation [14,15].

The optimization is started with an arbitrarily chosen initial control, $\phi^0 = (20^\circ, -40^\circ)$. It is shown in Fig. 2 that, after 6 iterations, the lift coefficient is improved by 18.7%, from 0.793 to 0.941. Three cases are compared in Table 1: (a) the rigid plate without trailing-edge flap, (b) the initial control, and (c) the optimal control, which are consistent with the choices of the direct parametric study by Li et al. [8]. The outcome of the adjoint-based optimization also matches very well with the direct parametric study. However, it is worth noting that the adjoint-based optimization (with 6 iterations) has much lower computational cost than the direct approach (with 72 cases). More important, the computational cost from the adjoint-based approach, by its nature, should remain at about the same level as the control parameters increase from 2 to a much larger number (e.g. more than 10); on the other hand, such increase of control parameters will lead to much larger (or impossible!) computational cost from the direct approach through the increase of cases to cover a much larger parametric space [14].

The optimal control provides much higher lift coefficient than the rigid case with 27% enhancement, though the initial control also provides lift enhancement by 7.3% from the rigid case. It is shown in Fig. 3 that, during one single flapping circle ($8T \le t < 9T$), the major lift enhancement happens at $t = 8.2T$ and $t = 8.8T$.